Electron-transfer-induced and phononic heat transport in molecular environments

Renai Chen,[1] Galen T. Craven,[1] and Abraham Nitzan[1,2,a)]
[1]*Department of Chemistry, University of Pennsylvania, Philadelphia, Pennsylvania 19104, USA*
[2]*School of Chemistry, Tel Aviv University, Tel Aviv 69978, Israel*

(Received 14 June 2017; accepted 29 August 2017; published online 25 September 2017)

A unified theory of heat transport in environments that sustain intersite phononic coupling and electron hopping is developed. The heat currents generated by both phononic transport and electron transfer between sites characterized by different local temperatures are calculated and compared. Using typical molecular parameters we find that the electron-transfer-induced heat current can be comparable to that of the standard phononic transport for donor-acceptor pairs with efficient bidirectional electron transfer rates (relatively small intersite distance and favorable free-energy difference). In most other situations, phononic transport is the dominant heat transfer mechanism. *Published by AIP Publishing.*
https://doi.org/10.1063/1.4990410

I. INTRODUCTION

The interplay between electric current and heat transfer drives energy conversion in diverse thermoelectric applications and results in a multitude of chemical functionalities which can be harnessed to perform operations in molecular devices, junctions, and machines.[1–10] Understanding the physical underpinnings of these processes and how they can be utilized for optimal functionality is a critical focus in nonequilibrium dynamics. In the regime where electron dynamics are strongly coupled with the motions of a surrounding thermal environment, charge transport between donor and acceptor molecules is dominated by hopping-type events, and electron transfer (ET) reactions can be described using the theory developed largely by Marcus,[11–17] Levich,[18] and Hush.[19–21] The so-called Marcus theory is a semiclassical theory that connects electron tunneling with transition state theory (TST)[16,22–27] and gives qualitative and sometimes quantitative predictions of reaction rates in the limit of strong electron-phonon coupling where a system's dynamical evolution can be described by electron occupation probabilities on the donor and acceptor sites. Multidimensional variants of Marcus theory have also been applied to cases where electron transport is coupled with other reactive coordinates, such as in proton-coupled electron transfer, and also to reactions that involve the transfer of multiple electrons.[28–37]

Energy (heat) transport in metals is dominated by electronic motion. By contrast, energy transport in molecular systems can occur through several channels depending on the form of energy transferred. Thermal energy (heat) transport is dominated by the phononic mechanism, i.e., the interaction and subsequent energy transfer between vibrational modes which are in contact with thermal environments of different temperatures.[38–49] In addition to studies that have elucidated the connection between composition, morphology, and microscopic structures of different environments and their heat conduction properties,[50–61] many recent studies have resulted in the development of molecular devices[56] such as thermal transistors[62–64] and thermal rectifiers[43,65,66] which use heat to perform useful functions and logical operations.

In contrast to metals, in the development of theories for charge and energy transport in molecular systems, a principal postulate is the absence of direct interdependence: charge transport takes place through electron transfer while heat transport occurs through phononic interactions. However, it has been recently shown that the transfer of electrons between a donor and acceptor whose environments are at different local temperatures generates a heat current solely from the electron transport.[67–69] In previous work, this ET-induced heat transport (ETIHT) has been examined between redox molecular motifs, at molecule-metal interfaces, and in molecular junctions using two significant approximations: (a) vibrational contributions to the total heat conduction were ignored to concentrate solely on the heat transport due to electron transfer and (b) the nuclear modes involved in the ET process were assumed to couple to, and to be in thermal equilibrium with, their local environments, e.g., the donor or acceptor neighborhood. Here, we augment this formalism to include vibrational heat transfer by allowing mode coupling to both sites. At steady state, each mode carries heat currents between the environments of different local temperatures to which it is coupled. At the same time, such modes promote electron transfer as described by the generalized Marcus theory of Refs. 67 and 68. This augmented theory allows direct comparison between the magnitude of the ET-induced and phononic heat conduction.

The remainder of the article is organized as follows: In Sec. II, we discuss details of the applied model and develop a unified theory for electron transfer, ETIHT, and phononic heat transfer by merging stochastic Langevin dynamics with multithermal Marcus theory. Section III contains the results obtained through application of the developed theory to different systems, with a specific focus placed on the

a)anitzan@sas.upenn.edu

interplay and magnitude comparison between phononic and electron-transfer-induced heat transport. Concluding remarks are given in Sec. IV, and the outlook for future work is also discussed.

II. THEORY OF MULTITHERMAL ELECTRON TRANSFER AND HEAT CONDUCTION

A. System details

To examine the relation between electron transfer and heat conduction as expressed by the ETIHT phenomenon, we apply a model that incorporates nonequilibrium Langevin-type stochastic dynamics into semiclassical Marcus-Levich ET theory.[11,12,16,70] The model is based on the Marcus-Levich picture of energy transfer in which a two-state (electron on donor and electron on acceptor) electronic system is coupled to N vibrational modes whose dynamics control the electron transfer. In departure from the Marcus-Levich picture, each mode is assumed to be in contact with two heat bath sites, denoted as a and b (we will henceforth take these to be the donor and acceptor sites) with respective local temperatures T_a and T_b. The motion of mode i is modeled by the Langevin equation,

$$\ddot{x}_i = -\gamma_a^{(i)}\dot{x}_i - \gamma_b^{(i)}\dot{x}_i - \frac{\partial \widetilde{E}_s(\boldsymbol{X})}{\partial x_i} + \xi_a^{(i)}(t) + \xi_b^{(i)}(t), \tag{1}$$

where $\boldsymbol{X} = \{x_1, \ldots, x_N\}$, $\widetilde{E}_s(\boldsymbol{X})$ is a mass-weighted energy surface whose geometry depends on the electronic state s of the system, $\gamma_a^{(i)}$ and $\gamma_b^{(i)}$ are coupling strengths to baths a and b, and $\xi_a^{(i)}(t)$ and $\xi_b^{(i)}(t)$ are stochastic noise terms of the respective bath. The stochastic terms obey the relations

$$\left\langle \xi_K^{(i)}(t)\xi_K^{(i)}(t')\right\rangle = 2\gamma_K^{(i)}k_{\mathrm{B}}T_K m_i^{-1}\delta(t-t'), \tag{2}$$

$$\left\langle \xi_a^{(i)}(t)\xi_b^{(i)}(t')\right\rangle = 0, \tag{3}$$

$$\left\langle \xi_K^{(i)}(t)\right\rangle = 0, \tag{4}$$

where $K \in \{a, b\}$ and $\langle \ldots \rangle$ denotes an average over the realizations of the noise. These correlations imply that the noise from each thermal source is white and is not correlated with the noise in the other bath or the noise in any other mode. The full dynamics of the system is described by N equations analogous to (1)—one for each mode—which are represented in a diagonal basis. However, electron transfer is a collective nuclear process involving all modes that are sensitive to the electronic occupations of the donor and acceptor sites. Consequently the modes interact through the geometrical modification of the underlying energy surface associated with the electronic states.

Here, electronic transport and ETIHT are modeled using a multithermal variant of Marcus ET theory.[67,68] The system has two electronic states: A and B, which correspond to electron localization on site a and site b, respectively. When the system is in electronic state A, the energy is

$$E_A(x_1, \ldots, x_N) = E_0^{(A)} + \sum_i^N \frac{1}{2}k_i\left(x_i - \lambda_i^{(A)}\right)^2, \tag{5}$$

and in electronic state B,

$$E_B(x_1, \ldots, x_N) = E_0^{(B)} + \sum_i^N \frac{1}{2}k_i\left(x_i - \lambda_i^{(B)}\right)^2, \tag{6}$$

where k_i is the force constant of the ith mode and $E_0^{(s)} : s \in \{A, B\}$ is the electronic energy origin of the respective state. The factors $\lambda_i^{(s)} : s \in \{A, B\}$ parameterize configurational changes in the environment of the respective mode due to electron localization on the corresponding site. The contribution to the total energy from the ith mode when the system is in the sth state is

$$E_s^{(i)}(x_i) = \frac{1}{2}k_i\left(x_i - \lambda_i^{(s)}\right)^2 : s \in \{A, B\}, \tag{7}$$

and each mode is characterized by a reorganization energy (which is the same for $A \to B$ and $B \to A$ transitions) given by

$$E_{\mathrm{R}i} = \frac{1}{2}k_i\left(\lambda_i^{(A)} - \lambda_i^{(B)}\right)^2. \tag{8}$$

The total reorganization energy for the electron transfer process is

$$E_{\mathrm{R}} = \sum_{i=1}^N E_{\mathrm{R}i}. \tag{9}$$

Each mode is in contact with two heat baths (a and b) with temperatures $T_a \neq T_b$; therefore, due to the thermal gradient, the system is intrinsically nonequilibrium even when electronic equilibrium (i.e., zero net electron transfer between the sites) has been reached. Solving the corresponding Fokker-Planck equation associated with Eq. (1)[38,39,46,47] yields that, at steady-state, each mode is characterized by an effective temperature,

$$T_i = \frac{\gamma_a^{(i)}T_a + \gamma_b^{(i)}T_b}{\gamma_a^{(i)} + \gamma_b^{(i)}}, \tag{10}$$

and the probability distribution in each mode will take a Gibbs form,

$$P_i \propto \exp\left[-\beta_i E_s^{(i)}(x_i)\right] : s \in \{A, B\}, \tag{11}$$

where $\beta_i = 1/k_{\mathrm{B}}T_i$, with k_{B} being Boltzmann's constant, and $E_s^{(i)}(x_i)$ is the energy of the ith mode [see Eq. (7)] in the sth state. Correspondingly, the total probability distribution for the system of N modes is

$$\begin{aligned} P &\propto \prod_{i=1}^N \exp\left[-\beta_i E_s^{(i)}(x_i)\right] \\ &\propto \prod_{i=1}^N \exp\left[-\frac{\gamma_a^{(i)} + \gamma_b^{(i)}}{k_{\mathrm{B}}(\gamma_a^{(i)}T_a + \gamma_b^{(i)}T_b)}E_s^{(i)}(x_i)\right], \end{aligned} \tag{12}$$

with $s \in \{A, B\}$, which illustrates that the distribution of each mode is characterized by the respective effective temperature of that particular mode.

B. Multithermal electron transfer theory

In Refs. 67 and 68, a theory was developed to treat multithermal ET reactions and this formalism can be adapted to treat the present model. The general form of the ET rate in the nonadiabatic limit is[16]

$$k_{A\to B} = \langle \mathcal{T}_{A\to B} v_\perp \rangle P_{A\to B}, \tag{13}$$

where $\mathcal{T}_{A\to B}$ is the tunneling probability from state A to B, $v_\perp$ is the velocity in the direction normal to a transition surface (TS) separating reactant and product regions, $P_{A\to B}$ is the probability density about the TS when the system is in state A, and $\langle\ldots\rangle$ denotes a multithermal average. The TS is defined by mode configurations that satisfy $g_c(x_1,\ldots,x_N) = E_B(x_1,\ldots,x_N) - E_A(x_1,\ldots,x_N) = 0$, which arises from the requirement that energy be conserved during an ET event.

The probability about the TS for the $A \to B$ transition is[67–69]

$$P_{A\to B} = \int_{\mathbb{R}^N}\prod_{i=1}^{N} dx_i \exp\left[\sum_{i=1}^{N} -\beta_i\frac{k_i}{2}\left(x_i-\lambda_i^{(A)}\right)^2\right] \times|\nabla g_c|\delta(g_c(x_1,\ldots,x_N)) \Big/ \int_{\mathbb{R}^N}\prod_{i=1}^{N} dx_i \exp\left[\sum_{i=1}^{N} -\beta_i\frac{k_i}{2}\left(x_i-\lambda_i^{(A)}\right)^2\right], \tag{14}$$

and for the $B \to A$ transition,

$$P_{B\to A} = \int_{\mathbb{R}^N}\prod_{i=1}^{N} dx_i \exp\left[\sum_{i=1}^{N} -\beta_i\frac{k_i}{2}\left(x_i-\lambda_i^{(B)}\right)^2\right] \times|\nabla g_c|\delta(g_c(x_1,\ldots,x_N)) \Big/ \int_{\mathbb{R}^N}\prod_{i=1}^{N} dx_i \exp\left[\sum_{i=1}^{N} -\beta_i\frac{k_i}{2}\left(x_i-\lambda_i^{(B)}\right)^2\right], \tag{15}$$

where the factor

$$|\nabla g_c| = \left(\sum_{i=1}^{N} 2k_i E_{\mathrm{R}i}\right)^{1/2} \tag{16}$$

ensures that the δ-function constraint is unique.[67,68,71] Evaluating the integrals yields

$$P_{A\to B} = \left(\frac{\sum_{i=1}^{N} k_i E_{\mathrm{R}i}}{2\pi k_{\mathrm{B}}\sum_{i=1}^{N} T_i E_{\mathrm{R}i}}\right)^{1/2} \exp\left[\frac{-(\Delta E_{BA}+E_{\mathrm{R}})^2}{4k_{\mathrm{B}}\sum_{i=1}^{N} T_i E_{\mathrm{R}i}}\right] \tag{17}$$

and

$$P_{B\to A} = \left(\frac{\sum_{i=1}^{N} k_i E_{\mathrm{R}i}}{2\pi k_{\mathrm{B}}\sum_{i=1}^{N} T_i E_{\mathrm{R}i}}\right)^{1/2} \exp\left[\frac{-(\Delta E_{BA}-E_{\mathrm{R}})^2}{4k_{\mathrm{B}}\sum_{i=1}^{N} T_i E_{\mathrm{R}i}}\right], \tag{18}$$

where $\Delta E_{BA} = -\Delta E_{AB} = E_0^{(B)} - E_0^{(A)}$ is the free energy difference between energy origins of the respective states for the $A \to B$ transition. The probability densities (and hence the ET reaction rates themselves) take the general forms derived in Refs. 67 and 68, but through their dependence on the effective temperatures also contain friction terms that arise from the Langevin description of the dynamics. Thus, the developed expressions for the multithermal ET transfer rate directly include terms that parameterize the coupling strengths to each bath.

The tunneling probability can be evaluated using the Landau-Zener approximation giving

$$\mathcal{T}_{A\to B} = \mathcal{T}_{\mathrm{LZ}} = 1 - \exp\left[-\frac{2\pi|V_{A,B}|^2}{\hbar|\Delta F|v_\perp}\right], \tag{19}$$

where $\hbar$ is the Planck constant, $|\Delta F| = |\nabla g_c|$ represents the force difference normal to the TS on the potential energy surface configuration, and $V_{A,B}$ is the energy coupling between diabatic surfaces. In the adiabatic limit, $\mathcal{T}_{\mathrm{LZ}} \to 1$, and in the nonadiabatic limit, a first-order approximation to (19) yields

$$\mathcal{T}_{\mathrm{LZ}} = \frac{2\pi|V_{A,B}|^2}{\hbar|\Delta F|v_\perp}. \tag{20}$$

In the nonadiabatic case, the expectation value $\langle\mathcal{T}_{A\to B}v_\perp\rangle$ is independent of the normal velocity and the expression for the ET rate from state A to state B is

$$k_{A\to B}^{(\mathrm{na})} = \frac{|V_{A,B}|^2}{\hbar|\Delta F|}\left(\frac{2\pi\sum_{i=1}^{N} k_i E_{\mathrm{R}i}}{k_{\mathrm{B}}\sum_{i=1}^{N} T_i E_{\mathrm{R}i}}\right)^{1/2} \exp\left[\frac{-(\Delta E_{BA}+E_{\mathrm{R}})^2}{4k_{\mathrm{B}}\sum_{i=1}^{N} T_i E_{\mathrm{R}i}}\right] \tag{21}$$

and from state B to state A is

$$k_{B\to A}^{(\mathrm{na})} = \frac{|V_{A,B}|^2}{\hbar|\Delta F|}\left(\frac{2\pi\sum_{i=1}^{N} k_i E_{\mathrm{R}i}}{k_{\mathrm{B}}\sum_{i=1}^{N} T_i E_{\mathrm{R}i}}\right)^{1/2} \exp\left[\frac{-(\Delta E_{BA}-E_{\mathrm{R}})^2}{4k_{\mathrm{B}}\sum_{i=1}^{N} T_i E_{\mathrm{R}i}}\right]. \tag{22}$$

The nonadiabatic rate constant is most relevant when the distance between donor and acceptor is large, and thus the energy coupling $V_{A,B}$ between diabats is small. We expect that this is the typical regime in which multithermal ET may be experimentally realizable because to hold the donor and acceptor environments at appreciable different temperatures requires such length scales. In the adiabatic limit, the rate is proportional to the average velocity in the normal direction to the TS,

$$k_{A\to B}^{(\mathrm{ad})} = \frac{\langle v_\perp\rangle}{2}P_{A\to B} \quad \text{and} \quad k_{B\to A}^{(\mathrm{ad})} = \frac{\langle v_\perp\rangle}{2}P_{B\to A}, \tag{23}$$

where the normal velocity is[68]

$$\langle v_\perp\rangle = \left(4k_{\mathrm{B}}\sum_{i=1}^{N} k_i T_i E_{\mathrm{R}i}\Big/\pi|\nabla g_c|^2 m_i\right)^{1/2}, \tag{24}$$

and a pre-factor 1/2 is included in (23) because, under standard TST assumptions, on an adiabatic surface only positive velocities contribute to the reactive flux and thus the reaction rate. In the case where $T_a = T_b$, the multithermal rates $k^{(\mathrm{na})}$ and $k^{(\mathrm{ad})}$ reduce to the standard Marcus expressions.[16,72]

C. Electron-transfer-induced heat transport (ETIHT)

Electron transfer across a thermal gradient can induce a net heat current between molecules,[67–69] and although we have a significant understanding of the physical manifestations underlying thermoelectric effects and phononic heat transport[6,49,73] in materials and molecular junctions,[2,8–10,74] the interplay between electronic and thermal currents is less understood when considering ETIHT effects in the strongly coupled

electron-phonon limit of transport. We have previously developed a theory for the heat current induced by electron transfer in thermal heterogeneous environments for a two-mode system in which each mode is in equilibrium with a single thermal reservoir, and the two reservoirs have different temperatures.[67] Here, we generalize that theory to the case of multiple modes whose evolution is governed by stochastic Langevin dynamics and each mode is coupled to multiple thermal baths.

Consider a vibrational mode i and denote a point on the TS along the corresponding coordinate by x_i^{TS}. To reach this point for the $A \to B$ transition, the mode needs to obtain energy $\mathcal{Q}_{Ai}^{\uparrow}$ from the baths during the ascent to x_i^{TS}. It will then release energy $\mathcal{Q}_{Bi}^{\downarrow}$ into the baths during the descent on the B surface after the electronic transition occurs. Similarly, for the $B \to A$ transition, the mode obtains energy $\mathcal{Q}_{Bi}^{\uparrow}$ from the baths during the ascent to the TS and then releases energy $\mathcal{Q}_{Ai}^{\downarrow}$ during the descent after the $B \to A$ electronic transition. The contribution of these modes to the energy change of the baths due to the process considered is thus given by

$$\begin{aligned}\mathcal{Q}_i^{A\to B} &\equiv -\mathcal{Q}_{Ai}^{\uparrow} + \mathcal{Q}_{Bi}^{\downarrow} \\ &= -\frac{1}{2}k_i\left(x_i^{\mathrm{TS}} - \lambda_i^{(A)}\right)^2 + \frac{1}{2}k_i\left(x_i^{\mathrm{TS}} - \lambda_i^{(B)}\right)^2, \quad (25)\\ \mathcal{Q}_i^{B\to A} &\equiv -\mathcal{Q}_{Bi}^{\uparrow} + \mathcal{Q}_{Ai}^{\downarrow} \\ &= -\frac{1}{2}k_i\left(x_i^{\mathrm{TS}} - \lambda_i^{(B)}\right)^2 + \frac{1}{2}k_i\left(x_i^{\mathrm{TS}} - \lambda_i^{(A)}\right)^2, \quad (26)\end{aligned}$$

where we have used the convention that energy released by the bath has a negative sign and energy obtained by the bath has a positive sign. A schematic of these energetics is shown in Fig. 1.

Electron transfer can occur at any configuration $\boldsymbol{X}$ on the TS; therefore, Eqs. (25) and (26) must be averaged of these configurations. It is important to note that in the multi-thermal situation considered here, the probability density to reach different configurations on the TS when coming from the A and B sides is not equal. These densities are given by[67]

$$\begin{aligned}P_{A\to B}^{\ddagger}(\boldsymbol{X}) = \delta(g_c)\exp\left[\sum_{i=1}^{N} -\beta_i\frac{k_i}{2}\left(x_i - \lambda_i^{(A)}\right)^2\right] \Big/ \int_{\mathbb{R}^N}\prod_i^N dx_i \\ \times\,\delta(g_c)\exp\left[\sum_{i=1}^{N} -\beta_i\frac{k_i}{2}\left(x_i - \lambda_i^{(A)}\right)^2\right], \quad (27)\end{aligned}$$

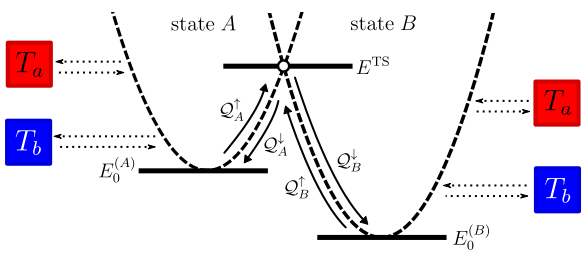

FIG. 1. Schematic of the energetics of heat exchange and energy partitioning between baths during the ascent to the transition state (shown as a circular marker) and the descent to the energy origin of the respective state. The dashed curves represent the energy surfaces E_A and E_B.

$$\begin{aligned}P_{B\to A}^{\ddagger}(\boldsymbol{X}) = \delta(g_c)\exp\left[\sum_{i=1}^{N} -\beta_i\frac{k_i}{2}\left(x_i - \lambda_i^{(B)}\right)^2\right] \Big/ \int_{\mathbb{R}^N}\prod_i^N dx_i \\ \times\,\delta(g_c)\exp\left[\sum_{i=1}^{N} -\beta_i\frac{k_i}{2}\left(x_i - \lambda_i^{(B)}\right)^2\right]. \quad (28)\end{aligned}$$

Averaging over all configurations on the TS using the corresponding probability densities, we find that the expectation values of the total heat transferred by mode i during the respective transitions are

$$\begin{aligned}\left\langle \mathcal{Q}_i^{A\to B}\right\rangle &= \int_{\mathbb{R}^N}\mathcal{Q}_i^{A\to B}P_{A\to B}^{\ddagger}(x_1,\ldots,x_N)dx_1\cdots dx_N \\ &= \frac{E_{\mathrm{R}i}\left[\Delta E_{AB}T_i + \sum_{k\neq i}^{N} E_{\mathrm{R}k}\left(T_k - T_i\right)\right]}{\sum_k^N T_k E_{\mathrm{R}k}} \quad (29)\end{aligned}$$

and

$$\begin{aligned}\left\langle \mathcal{Q}_i^{B\to A}\right\rangle &= \int_{\mathbb{R}^N}\mathcal{Q}_i^{B\to A}P_{B\to A}^{\ddagger}(x_1,\ldots,x_N)dx_1\cdots dx_N \\ &= -\frac{E_{\mathrm{R}i}\left[\Delta E_{AB}T_i - \sum_{k\neq i}^{N} E_{\mathrm{R}k}\left(T_k - T_i\right)\right]}{\sum_k^N T_k E_{\mathrm{R}k}}. \quad (30)\end{aligned}$$

Equations (29) and (30) are expressions for the net heat exchange associated with mode i in the corresponding ET processes. In Ref. 67, knowledge of these quantities was sufficient for calculating the heat transfer between baths because each mode was coupled only to a single bath. Here, however, the mode can be coupled to both baths, and to obtain the net heat exchange by such modes requires knowledge of the energy partitioning between baths. Specifically, we require an answer to the following question: If the net heat exchange with the baths (accumulated during ascent plus released during descent) is $\mathcal{Q}$, how is $\mathcal{Q}$ partitioned between the two baths?

A guide to how this partitioning works can be obtained from the following argument. From the kinetic master equations of a two-level system with energy level spacing ΔE that is coupled to two baths, we find that the fraction of energy ΔE_K that is obtained/released by the Kth bath during a state transition is

$$\Delta E_K = \frac{\gamma_K\langle n_K\rangle}{\gamma_a\langle n_a\rangle + \gamma_b\langle n_b\rangle}\Delta E : K \in \{a,b\}, \quad (31)$$

where

$$\langle n_K(\Delta E)\rangle = \frac{1}{e^{\beta_K\Delta E} - 1} \quad (32)$$

is the quantum population in equilibrium with the respective thermal bath. In the classical limit $\langle n_K\rangle \sim T_K$ and, thus, in the limit where the Langevin dynamics of Eq. (1) adequately describe the system's evolution,

$$\Delta E_K = \frac{\gamma_K T_K}{\gamma_a T_a + \gamma_b T_b}\Delta E : K \in \{a,b\}, \quad (33)$$

which states that bath K provides/absorbs $\gamma_K T_K/(\gamma_a T_a + \gamma_b T_b)$ of the total energy change during each transition.

A more rigorous derivation of Eq. (33) for the Langevin dynamics considered here will be provided elsewhere. Using

this partitioning during both activation and relaxation events, we arrive at general expressions for the heat current generated into each bath at steady state solely from the transfer of electrons across a thermal gradient,

$$J_{\mathcal{Q}}^{(a)} = J_{\rm el}\sum_i^N \frac{\gamma_a^{(i)}T_a}{\gamma_a^{(i)}T_a+\gamma_b^{(i)}T_b}\left(\langle \mathcal{Q}_i^{A\to B}\rangle + \langle \mathcal{Q}_i^{B\to A}\rangle\right),$$
$$= 2J_{\rm el}\sum_i^N \frac{\gamma_a^{(i)}T_a}{\gamma_a^{(i)}T_a+\gamma_b^{(i)}T_b}\left[\frac{E_{{\rm R}i}\sum_{k\neq i}^N E_{{\rm R}k}\,(T_k-T_i)}{\sum_k^N T_k E_{{\rm R}k}}\right], \quad (34)$$

$$J_{\mathcal{Q}}^{(b)} = J_{\rm el}\sum_i^N \frac{\gamma_b^{(i)}T_b}{\gamma_a^{(i)}T_a+\gamma_b^{(i)}T_b}\left(\langle \mathcal{Q}_i^{A\to B}\rangle + \langle \mathcal{Q}_i^{B\to A}\rangle\right)$$
$$= 2J_{\rm el}\sum_i^N \frac{\gamma_b^{(i)}T_b}{\gamma_a^{(i)}T_a+\gamma_b^{(i)}T_b}\left[\frac{E_{{\rm R}i}\sum_{k\neq i}^N E_{{\rm R}k}\,(T_k-T_i)}{\sum_k^N T_k E_{{\rm R}k}}\right], \quad (35)$$

where $J_{\rm el}$ is the unidirectional electronic current at steady state. In this state, the electronic system has reached quasi-equilibrium where the electronic state populations $p_K^{(\rm ss)} : K \in \{A, B\}$ do not change so that

$$J_{A\to B}^{(\rm ss)} = J_{B\to A}^{(\rm ss)} \equiv J_{\rm el} = p_A^{(\rm ss)}k_{A\to B}, \quad (36)$$

where $p_A^{(\rm ss)}$ is the steady state probability that the system is in electronic state A. It is easily confirmed that these currents satisfy the energy conservation condition $J_{\mathcal{Q}}^{(a)} = -J_{\mathcal{Q}}^{(b)}$.

Some insight on these results can be obtained by considering special cases. Consider first a system with a single vibrational mode that is coupled to sites a and b. The total heat energies transferred between the baths during the and $A \to B$ and $B \to A$ transitions are

$$\left\langle \mathcal{Q}_i^{A\to B}\right\rangle = \Delta E_{AB}, \quad (37)$$
$$\left\langle \mathcal{Q}_i^{B\to A}\right\rangle = -\Delta E_{AB}, \quad (38)$$

where E_{AB} is the free energy difference between the two electronic states. These energies cancel each other when summed to yield the total heat associated with a "round trip" between the states; therefore, there is no ET-induced heat current for a single mode coupled to two thermal sources. One way to understand the reason for this is to note that the single mode is associated with a single effective temperature, so the electron transfer process is not subjected to a temperature difference between the thermal baths. Obviously, such a single mode, being coupled to two baths of different temperatures, will contribute to the standard (phononic) heat transport (see Sec. II D).

Next consider a two-mode system. Equations (34) and (35) now yield

$$J_{\mathcal{Q}} = J_{\mathcal{Q}}^{(a)} = -J_{\mathcal{Q}}^{(b)} = 2J'_{\rm el}\frac{E_{\rm R1}E_{\rm R2}\,(T_2-T_1)}{T_1E_{\rm R1}+T_2E_{\rm R2}}, \quad (39)$$

where

$$J'_{\rm el} = J_{\rm el}\frac{T_aT_b\left(\gamma_a^{(1)}\gamma_b^{(2)}-\gamma_a^{(2)}\gamma_b^{(1)}\right)}{\left(\gamma_a^{(1)}T_a+\gamma_b^{(1)}T_b\right)\left(\gamma_a^{(2)}T_a+\gamma_b^{(2)}T_b\right)}, \quad (40)$$

which has the same form as derived in Ref. 67, except that now the temperatures T_1 and T_2 and the flux $J'_{\rm el}$ are effective quantities that depend on the different system-bath coupling strengths.

It is interesting to realize that at least two vibrational modes, characterized by different effective temperatures and sensitive to the electronic site occupations, are needed for ETIHT. Also notable is the nonlinear dependence of this effect on the temperature difference between baths and the system-bath couplings. Aside from the system-bath coupling terms which appear explicitly in Eqs. (34) and (35), the steady state unidirectional electron current $J_{\rm el}$ is also determined by the ET rates, which themselves are affected by these couplings. We study these dependences in Sec. III.

D. Vibrational heat transfer

For a single harmonic mode i coupled to two thermal baths a and b according to the Langevin equations (1)–(4), the vibrational heat current is[38]

$$J_{\mathcal{Q}_i}^{(a)} = -J_{\mathcal{Q}_i}^{(b)} = k_{\rm B}\frac{\gamma_a^{(i)}\gamma_b^{(i)}}{\gamma_a^{(i)}+\gamma_b^{(i)}}(T_b-T_a). \quad (41)$$

Equation (41) is a classical high temperature ($k_{\rm B}T \gg \hbar\omega_i$) limit of a more general quantum result,[43] which for $k_{\rm B}T \gg \hbar\gamma_i$ takes the form

$$J_{\mathcal{Q}_i}^{(a)} = -J_{\mathcal{Q}_i}^{(b)} = \hbar\omega\frac{\gamma_a^{(i)}\gamma_b^{(i)}}{\gamma_a^{(i)}+\gamma_b^{(i)}}(n_b-n_a), \quad (42)$$

with

$$n_K \equiv \langle n_K\rangle = \frac{e^{-\beta_K\hbar\omega}}{(1-e^{-\beta_K\hbar\omega})}, \quad (43)$$

where $K \in \{a, b\}$ and $\langle\cdots\rangle$ is a thermal average. In the classical limit, the total vibrational heat current is given by the sum over modes,

$$J_{\mathcal{Q}}^{(a)} = -J_{\mathcal{Q}}^{(b)} = k_{\rm B}(T_b-T_a)\sum_{i=1}^N \frac{\gamma_a^{(i)}\gamma_b^{(i)}}{\gamma_a^{(i)}+\gamma_b^{(i)}}. \quad (44)$$

The contribution of each mode depends on the temperature difference between baths, weighted by the mode-bath coupling strength.

Next, we apply these results to estimate the relative importance of the vibrational and ET-induced heat conductivities in molecular systems.

III. RESULTS AND DISCUSSION

To gain insights into the interplay between ETIHT and purely vibrational contributions to heat transport, we consider a system of two electronic sites and two vibrational modes (in which both ETIHT and phononic heat transport can be observed) with the following attributes: mode 1 is assumed to be preferably localized near site a, so its coupling to the thermal environment near this site is stronger than its coupling to the environment of site b. Conversely, mode 2 is more localized about site b and therefore is more strongly coupled to that site. This also implies that mode 1 may be more sensitive to the electronic occupation of site a while mode 2 is more affected by the electronic occupation on site b, but this difference does

not affect the way these modes are expressed in the electron transfer rate between these sites because their effect enters through the symmetric coupling $\left(\lambda^{(A)} - \lambda^{(B)}\right)^2$.

In the model considered here, the coupling between the electronic and vibrational subsystems maintains the character of the vibrational modes in the two electronic states, and thus the two heat transfer channels, vibrational and ETIHT, operate additively. The electron transfer process depends of course on the effective vibrational temperatures; however, the vibrational heat transport is not affected by the electron transfer and is independent of molecular parameters that affect the electron transfer, such as the reorganization energies and the free energy difference between the electronic states. The relative importance of these channels as determined by their contributions to the heat transfer is therefore derived from their essentially independent efficiencies.

Figure 2 illustrates how the heat current from the ETIHT and phononic conduction channels vary with changing reaction free energy ΔE_{BA} and the coupling of the vibrational modes to the thermal environments of the donor and acceptor. The parameters for this calculation are chosen such that the γ values are in the range of typical vibrational relaxation rates for large molecules in condensed-phases at room temperature and the total reorganization energy E_R is on the order of values observed in ET reactions in polar solvents. We also note that the effective energy transmission coefficient $\frac{\gamma_a^{(i)}\gamma_b^{(i)}}{\gamma_a^{(i)}+\gamma_b^{(i)}}$ of Eq. (41) can be roughly estimated to be around 0.1–1 ps^{-1} from thermal conductance measurements of alkane chains under standard

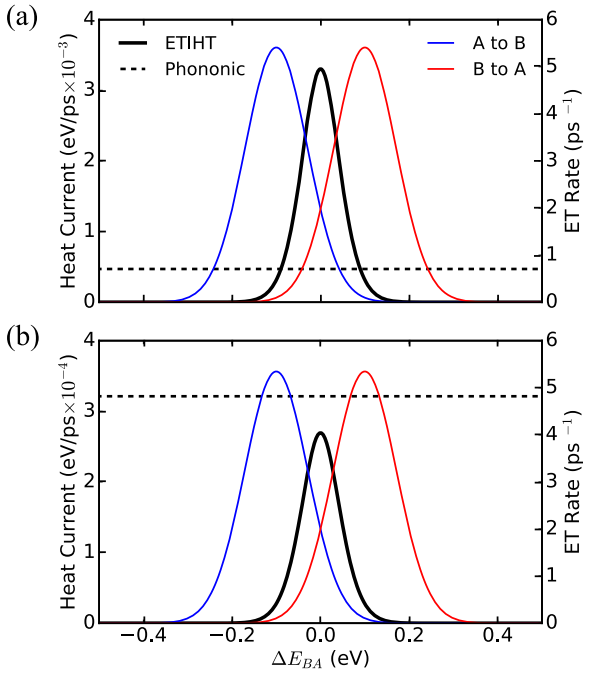

FIG. 2. Electron-transfer-induced (solid, black) and phononic (dashed, black) heat currents $\mathcal{J}_Q$ (current direction from left to right) and electron transfer rates $k_{A\to B}$ (solid, blue) and $k_{B\to A}$ (solid; red) as functions of the free energy difference ΔE_{BA}. Units and scale of the heat currents and electron transfer rates are shown on the left and right axes, respectively. The system-bath couplings are $\gamma_a^{(1)} = 1.0$ ps^{-1}, $\gamma_b^{(1)} = 0.1$ ps^{-1}, and $\gamma_a^{(2)} = 0.1$ ps^{-1} in both panels; (a) $\gamma_b^{(2)} = 1.0$ ps^{-1} and (b) $\gamma_b^{(2)} = 0.05$ ps^{-1}. Other parameters are $V_{A,B} = 0.01$ eV, $E_{R1} = 0.06$ eV, $E_{R2} = 0.04$ eV, $T_a = 300$ K, and $T_b = 270$ K.

conditions,[42] and the values used here are on this order. We choose the relations between parameter values to illustrate a comparison between electron-transfer-induced heat transport and vibrational heat transfer for a two-mode model for several physically relevant limiting cases. Specifically, in Fig. 2(a) the coupling strength of mode 1 to site a is ten times larger than its coupling to site b, i.e., $\gamma_a^{(1)} = 10\gamma_b^{(1)}$, and the coupling strength of mode 2 to site a is ten times less than its coupling to site b, i.e., $10\gamma_a^{(2)} = \gamma_b^{(2)}$. In Fig. 2(b), both modes are strongly coupled to site a and weakly coupled to site b. This is a different limiting case in which each mode is strongly coupled to the same local environment.

The following observations can be made:

(a) In the parameter ranges examined here, the vibrational heat conduction is $\sim 5 \times 10^{-4}$ eV/ps, which is within the range of the heat current magnitude measured by state-of-the-art experimental technique in molecular junctions.[75,76] This also indicates that an electron-transfer-induced heat current could be detected experimentally. A specific case where ETIHT could be the dominant conduction mechanism is in molecular junctions in which the phononic heat current is effectively suppressed due to the electronic characteristics of the molecular structure.[77]

(b) As explained above, and as seen in Fig. 2, the phononic heat current does not depend on ΔE_{BA}. In contrast, the dependence of the ETIHT on this parameter is dramatic—it peaks at $\Delta E_{BA} = 0$ and dies down quickly as $|\Delta E_{BA}|$ is increased. This behavior reflects the fact that ETIHT depends on the rate of electron transfer in both directions and is therefore maximum when rates for both the $D \to A$ and $A \to D$ processes are appreciable rather than when one rate dominates the other.

(c) The couplings between the oscillator modes and the thermal environments of the electronic centers influence the heat transport between these centers as seen in Fig. 2. Its effect on the phononic part of the heat current is obvious, and an important effect on the electron transfer rate results from the fact that the latter depends on the effective temperatures that depend on these couplings. Another important effect of these couplings on the relative magnitudes of the ETIHT and the purely vibrational contributions stems from their symmetry properties. In panel (b) of Fig. 2, the coupling of the mode 2 to the bath b is decreased by a factor of two with respect to panel (a) and the ETIHT current goes down by nearly an order of magnitude. The origin of this behavior lies in the symmetry properties of the coupling parameters. Figure 2(a) refers to the case where one mode is strongly coupled to site a while the other mode is strongly coupled to site b, as compared to Fig. 2(b) where both modes are coupled more strongly to site a. It is the former scenario that gives the strongest ETIHT effect. In the limit in which one mode is coupled only to site a while the other sees only site b, i.e., $\gamma_b^{(1)} = \gamma_a^{(2)} = 0$, there is no direct vibrational coupling between the thermal environments of sites a and b and the total contribution to the heat transport comes solely from the ETIHT channel. In

another special limit where the ratios of the couplings satisfy the equality

$$\frac{\gamma_a^{(1)}}{\gamma_a^{(2)}} = \frac{\gamma_b^{(1)}}{\gamma_b^{(2)}} \quad \text{or} \quad \frac{\gamma_a^{(1)}}{\gamma_b^{(1)}} = \frac{\gamma_a^{(2)}}{\gamma_b^{(2)}}, \tag{45}$$

the ETIHT contribution to the heat current is zero while the phononic counterpart is nonzero and proportional to the temperature difference between sites.

Figure 3 shows the dependence of these heat transport channels on the temperature difference between the donor and acceptor sites. Variation of $\Delta T = T_a - T_b$ seen in Fig. 3 for various constant ΔE_{BA} values is expressed differently in the different heat transport channels. While the phononic heat current increases linearly with ΔT, increasing the temperature difference between baths does not linearly add to the magnitude of the ETIHT current. Figure 3 illustrates these behaviors for different sets of system-bath couplings.

A corollary of this observation is that while the phononic heat current depends linearly on ΔT, the non-linear response of the ETIHT current may lead to situations (usually at small ΔT) which it exceeds its phononic counterpart. For instance, in the $\Delta E_{BA} = 0.1$ eV case in Fig. 3(a), the ETIHT current is less than the phononic current for small temperature biases, while for $\Delta T > 150$ K, the ETIHT current is greater than that generated in the phononic channel. These results imply that by tuning the coupling strength between donor and acceptor molecules and their local environments,

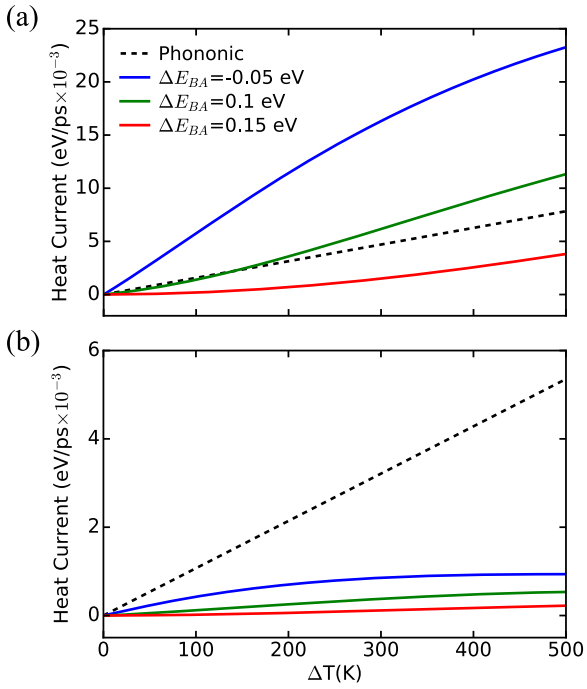

FIG. 3. Electron-transfer-induced and phononic heat currents $\mathcal{J}_Q$ (current direction from left to right) as a function of temperature difference $\Delta T = T_a - T_b$ for various values of the reaction free energy ΔE_{BA} shown in the legend of (a). The system-bath couplings are $\gamma_a^{(1)} = 1.0\ \text{ps}^{-1}$, $\gamma_b^{(1)} = 0.1\ \text{ps}^{-1}$, and $\gamma_a^{(2)} = 0.1\ \text{ps}^{-1}$ in both panels; (a) $\gamma_b^{(2)} = 1.0\ \text{ps}^{-1}$ and (b) $\gamma_b^{(2)} = 0.05\ \text{ps}^{-1}$. Other parameters are $V_{A,B} = 0.01$ eV, $E_{\text{R1}} = 0.06$ eV, $E_{\text{R2}} = 0.04$ eV, and $T_b = 270$ K, which are fixed.

the comparative magnitude of ETIHT current can be increased over that of phononic heat current in some multithermal ET reactions.

IV. CONCLUSIONS

In this article, we have developed a theory to describe electron transfer between environments with different local temperatures and phononic heat conduction between these environments using a multithermal Marcus formalism merged with stochastic Langevin dynamics. Coupling between the thermal fluctuations of each site's local environment and the electron gives rise to electron-transfer-induced heat transport (ETIHT). Application of this theory allows a comparison between the magnitude of heat conduction from phononic and electron-transfer-induced channels over a diverse set of reaction geometries and thermal environments. An efficient ETIHT channel requires fast bidirectional electron exchange between the molecular sites, which usually translates into the requirement that the free energy change associated with the electron transfer reaction is small, such as in the case of exchange between identical sites. In such cases, situations could be found where this channel dominates the heat transport process; however, this conclusion should be taken cautiously because the comparison performed here is most valid for modes that are strongly coupled to both thermal environments and at the same time are also coupled to the electron transfer process. Other heat carrying modes may be uncoupled to the electronic process. Obviously there are also modes that couple to the electronic process but do not carry heat (in the harmonic limit) because they are localized near their respective environments. We note in passing that the harmonic part of the nuclear potential energy surface indeed dominates heat transport across distance scales that are relevant for the present study.[42]

A system in which ETIHT could be the dominant thermal conduction mechanism is π-stacked molecular junctions where the phononic transport channel is suppressed by tuning specific bonding characteristics of the molecular structure.[77] In the limit that electron charge density is strongly coupled with a thermal environment, the results presented here will guide experimental investigation of ETIHT.

Apart from the harmonic approximation, the developed formalism relies on two assumptions. First is the assumed independence of the ETIHT and the phononic contributions to heat transfer. This assumption is valid in the limit in which the vibrational transport mechanism does not affect the energetic distributions relevant to electron transport. This holds at steady state for the standard model of electron transfer (parallel shifted potential energy surfaces) except that the temperature associated with the relevant nuclear motions has to be set as the effective temperature derived for each mode from its coupling to the non-equilibrium environment. Second is an assumption concerning the partitioning of energy extracted from and released into the non-equilibrium thermal baths during the activated electron transfer process. This assumption, expressed by Eq. (33) is derived from a master equation approach. We are currently developing a theory of the energy partitioning from a trajectory-based picture of the dynamics, and our preliminary

results agree with the energy partitioning principle derived from the kinetic master equations.

Finally we note that the semiclassical formalism that has been implemented here is applicable for low frequency intermolecular vibrations in the strong electron-phonon coupling limit in which electron hopping is the dominant transport mechanism. At low temperatures, and for high frequency molecular vibrations, nuclear tunneling plays a role in the system's dynamical evolution, and a description of ETIHT will require a quantum description of the nuclear dynamics. Carrying the theory to such situation is a focus of our current work.

ACKNOWLEDGMENTS

The research of A.N. is supported by the US-Israel Binational Science Foundation, the German Research Foundation (DFG TH 820/11-1), the U.S. National Science Foundation (Grant No. CHE1665291), and the University of Pennsylvania.

[1] P. Reddy, S.-Y. Jang, R. A. Segalman, and A. Majumdar, Science **315**, 1568 (2007).
[2] K. Walczak, Physica B **392**, 173 (2007).
[3] J. A. Malen, P. Doak, K. Baheti, T. D. Tilley, A. Majumdar, and R. A. Segalman, Nano Lett. **9**, 3406 (2009).
[4] J. A. Malen, S. K. Yee, A. Majumdar, and R. A. Segalman, Chem. Phys. Lett. **491**, 109 (2010).
[5] A. Tan, J. Balachandran, S. Sadat, V. Gavini, B. D. Dunietz, S.-Y. Jang, and P. Reddy, J. Am. Chem. Soc. **133**, 8838 (2011).
[6] J. Ren, J.-X. Zhu, J. E. Gubernatis, C. Wang, and B. Li, Phys. Rev. B **85**, 155443 (2012).
[7] Y. Kim, W. Jeong, K. Kim, W. Lee, and P. Reddy, Nat. Nanotechnol. **9**, 881 (2014).
[8] T. Koch, J. Loos, and H. Fehske, Phys. Rev. B **89**, 155133 (2014).
[9] C. A. Perroni, D. Ninno, and V. Cataudella, Phys. Rev. B **90**, 125421 (2014).
[10] N. A. Zimbovskaya, J. Phys.: Condens. Matter **26**, 275303 (2014).
[11] R. A. Marcus, J. Chem. Phys. **24**, 966 (1956).
[12] R. A. Marcus, Annu. Rev. Phys. Chem. **15**, 155 (1964).
[13] R. A. Marcus and N. Sutin, Biochim. Biophys. Acta **811**, 265 (1985).
[14] R. A. Marcus, Rev. Mod. Phys. **65**, 599 (1993).
[15] M. Tachiya, J. Phys. Chem. **97**, 5911 (1993).
[16] A. Nitzan, *Chemical Dynamics in Condensed Phases: Relaxation, Transfer and Reactions in Condensed Molecular Systems* (Oxford University Press, 2006).
[17] B. Peters, J. Phys. Chem. B **119**, 6349 (2015).
[18] A. M. Kuznetsov and J. Ulstrup, *Electron Transfer in Chemistry and Biology: An Introduction to the Theory* (John Wiley & Sons, Ltd., 1999).
[19] N. Hush, J. Chem. Phys. **28**, 962 (1958).
[20] N. Hush, Trans. Faraday Soc. **57**, 557 (1961).
[21] N. Hush, Electrochim. Acta **13**, 1005 (1968).
[22] D. G. Truhlar, B. C. Garrett, and S. J. Klippenstein, J. Phys. Chem. **100**, 12771 (1996).
[23] T. Komatsuzaki and R. S. Berry, Proc. Natl. Acad. Sci. U. S. A. **98**, 7666 (2001).
[24] T. Bartsch, R. Hernandez, and T. Uzer, Phys. Rev. Lett. **95**, 058301(1) (2005).
[25] R. Hernandez, T. Bartsch, and T. Uzer, Chem. Phys. **370**, 270 (2010).
[26] G. T. Craven, T. Bartsch, and R. Hernandez, Phys. Rev. E **89**, 040801(R) (2014).
[27] G. T. Craven and R. Hernandez, Phys. Rev. Lett. **115**, 148301 (2015).
[28] M. Tachiya, J. Phys. Chem. **93**, 7050 (1989).
[29] M. Steeger, S. Griesbeck, A. Schmiedel, M. Holzapfel, I. Krummenacher, H. Braunschweig, and C. Lambert, Phys. Chem. Chem. Phys. **17**, 11848 (2015).
[30] A. V. Soudackov, A. Hazra, and S. Hammes-Schiffer, J. Chem. Phys. **135**, 144115 (2011).
[31] S. Hammes-Schiffer, J. Am. Chem. Soc. **137**, 8860 (2015).
[32] A. K. Harshan, T. Yu, A. V. Soudackov, and S. Hammes-Schiffer, J. Am. Chem. Soc. **137**, 13545 (2015).
[33] E. Grunwald, J. Am. Chem. Soc. **107**, 125 (1985).
[34] J. P. Guthrie, J. Am. Chem. Soc. **118**, 12878 (1996).
[35] C. Lambert, G. Nöll, and F. Hampel, J. Phys. Chem. A **105**, 7751 (2001).
[36] J. Zwickl, N. Shenvi, J. R. Schmidt, and J. C. Tully, J. Phys. Chem. A **112**, 10570 (2008).
[37] I. V. Rubtsov, Nat. Chem. **7**, 683 (2015).
[38] J. L. Lebowitz, Phys. Rev. **114**, 1192 (1959).
[39] Z. Rieder, J. L. Lebowitz, and E. Lieb, J. Math. Phys. **8**, 1073 (1967).
[40] A. Casher and J. L. Lebowitz, J. Math. Phys. **12**, 1701 (1971).
[41] K. Sekimoto, Prog. Theor. Phys. Suppl. **130**, 17 (1998).
[42] D. Segal, A. Nitzan, and P. Hänggi, J. Chem. Phys. **119**, 6840 (2003).
[43] D. Segal and A. Nitzan, Phys. Rev. Lett. **94**, 034301 (2005).
[44] A. Dhar and J. L. Lebowitz, Phys. Rev. Lett. **100**, 134301 (2008).
[45] V. Kannan, A. Dhar, and J. L. Lebowitz, Phys. Rev. E **85**, 041118 (2012).
[46] S. Sabhapandit, Phys. Rev. E **85**, 021108 (2012).
[47] A. Dhar and R. Dandekar, Physica A **418**, 49 (2015).
[48] K. A. Velizhanin, S. Sahu, C.-C. Chien, Y. Dubi, and M. Zwolak, Sci. Rep. **5**, 17506 (2015).
[49] Y. Murashita and M. Esposito, Phys. Rev. E **94**, 062148 (2016).
[50] D. G. Cahill, K. Goodson, and A. Majumdar, J. Heat Transfer **124**, 223 (2002).
[51] D. G. Cahill, W. K. Ford, K. E. Goodson, G. D. Mahan, A. Majumdar, H. J. Maris, R. Merlin, and S. R. Phillpot, J. Appl. Phys. **93**, 793 (2003).
[52] M. Galperin, A. Nitzan, and M. A. Ratner, Phys. Rev. B **75**, 155312 (2007).
[53] D. M. Leitner, Annu. Rev. Phys. Chem. **59**, 233 (2008).
[54] D. M. Leitner, Adv. Phys. **64**, 445 (2015).
[55] Q. Li, I. Duchemin, S. Xiong, G. C. Solomon, and D. Donadio, J. Phys. Chem. C **119**, 24636 (2015).
[56] N. Li, J. Ren, L. Wang, G. Zhang, P. Hänggi, and B. Li, Rev. Mod. Phys. **84**, 1045 (2012).
[57] N. Yang, X. Xu, G. Zhang, and B. Li, AIP Adv. **2**, 041410 (2012).
[58] A. Dhar, Adv. Phys. **57**, 457 (2008).
[59] T. Luo and G. Chen, Phys. Chem. Chem. Phys. **15**, 3389 (2013).
[60] N. I. Rubtsova, L. N. Qasim, A. A. Kurnosov, A. L. Burin, and I. V. Rubtsov, Acc. Chem. Res. **48**, 2547 (2015).
[61] N. I. Rubtsova, C. M. Nyby, H. Zhang, B. Zhang, X. Zhou, J. Jayawickramarajah, A. L. Burin, and I. V. Rubtsov, J. Chem. Phys. **142**, 212412 (2015).
[62] B. Li, L. Wang, and G. Casati, Appl. Phys. Lett. **88**, 143501 (2006).
[63] P. Ben-Abdallah and S.-A. Biehs, Phys. Rev. Lett. **112**, 044301 (2014).
[64] K. Joulain, J. Drevillon, Y. Ezzahri, and J. Ordonez-Miranda, Phys. Rev. Lett. **116**, 200601 (2016).
[65] M. Terraneo, M. Peyrard, and G. Casati, Phys. Rev. Lett. **88**, 094302 (2002).
[66] C. Chang, D. Okawa, A. Majumdar, and A. Zettl, Science **314**, 1121 (2006).
[67] G. T. Craven and A. Nitzan, Proc. Natl. Acad. Sci. U. S. A. **113**, 9421 (2016).
[68] G. T. Craven and A. Nitzan, Phys. Rev. Lett. **118**, 207201 (2017).
[69] G. T. Craven and A. Nitzan, J. Chem. Phys. **146**, 092305 (2017).
[70] M. D. Newton and N. Sutin, Annu. Rev. Phys. Chem. **35**, 437 (1984).
[71] C. Hartmann, J. C. Latorre, and G. Ciccotti, Eur. Phys. J.: Spec. Top. **200**, 73 (2011).
[72] J. O. Richardson and M. Thoss, J. Chem. Phys. **141**, 074106 (2014).
[73] M. Esposito, M. A. Ochoa, and M. Galperin, Phys. Rev. B **91**, 115417 (2015).
[74] J. S. Lim, R. López, and D. Sánchez, Phys. Rev. B **88**, 201304 (2013).
[75] T. Meier, F. Menges, P. Nirmalraj, H. Hölscher, H. Riel, and B. Gotsmann, Phys. Rev. Lett. **113**, 060801 (2014).
[76] Z. Wang, J. A. Carter, A. Lagutchev, Y. K. Koh, N.-H. Seong, D. G. Cahill, and D. D. Dlott, Science **317**, 787 (2007).
[77] Q. Li, M. Strange, I. Duchemin, D. Donadio, and G. C. Solomon, J. Phys. Chem. C **121**, 7175–7182 (2017).